



*William R. Wiley*

**EMSL**

Environmental Molecular Sciences Laboratory

**EMSL Report**  
**June 2007 – July 2007**

---

The W.R. Wiley Environmental Molecular Sciences Laboratory (EMSL) is a U.S. Department of Energy (DOE) national scientific user facility located at Pacific Northwest National Laboratory (PNNL) in Richland, Washington. EMSL is operated by PNNL for the DOE Office of Biological and Environmental Research. At one location, EMSL offers a comprehensive array of leading-edge resources in six research facilities.

Access to the capabilities and instrumentation in EMSL facilities is obtained on a peer-reviewed proposal basis, and users are participants on accepted proposals. EMSL staff members work with users to expedite access to the research facilities, support capabilities, and the resident scientific expertise. The bimonthly report documents research and activities of EMSL staff and users.

## Research Highlights

### Doping Golden Buckyballs: $\text{Cu@Au}_{16}^-$ and $\text{Cu@Au}_{17}^-$ Cluster Anions

**LM Wang,<sup>(a)</sup> S Bulusu,<sup>(b)</sup> HJ Zhai,<sup>(a)</sup> XC Zeng,<sup>(b)</sup> and LS Wang<sup>(a)</sup>**

**(a) Washington State University Tri-Cities, Richland Washington**

**(b) University of Nebraska, Lincoln, Nebraska**

*Clusters are groups of a small number of atoms that often have chemical and physical properties that are different than the corresponding bulk materials. Understanding the underlying physical and structural reasons for these unique properties may allow for improved materials for electronics, sensors, and catalysis.*

The discovery of the unique catalytic effects of gold nanoparticles on oxide substrates has stimulated a flurry of research into the structures and properties of free gold nanoclusters, which may hold the key to elucidating the catalytic mechanisms of supported gold clusters. One of the most remarkable results has been the discovery of planar gold cluster anions ( $\text{Au}_n^-$ ) of up to 12 gold atoms and the two- to three-dimensional transition for clusters with  $n$  larger than 12. Among larger gold clusters,  $\text{Au}_{20}$  has been found to be a perfect tetrahedron. A more recent study of the structures of  $\text{Au}_n^-$  cluster anions in the medium size range ( $n=15-19$ ) has shown that clusters with  $n=16-18$  possess unprecedented empty cage structures. In particular, the  $\text{Au}_{16}^-$  cluster anion has an interesting tetrahedral structure with an inner diameter of about 5.5 Å and can be compared to the fullerenes (buckyballs). The cage structures of the cluster anions  $\text{Au}_{16}^-$  and  $\text{Au}_{17}^-$  have recently been confirmed by electron diffraction, and thus, they are the first experimentally confirmed and the smallest possible gold cages. The large empty space inside these cage clusters immediately suggested that they can be doped with a foreign atom to produce a new class of endohedral gold cages that are analogous to endohedral fullerenes.

A gold cage containing a central atom first was predicted for a series of icosahedral clusters  $\text{M@Au}_{12}$  ( $\text{M}=\text{W}, \text{Ta}, \text{Re}^+$ ) based on the 18-electron rule and subsequently was confirmed experimentally. However, because  $\text{Au}_{12}$  itself does not possess a cage structure, the dopant atom with the appropriate electron count must play an essential role in maintaining the integrity of the cage. Bimetallic gold clusters have been studied experimentally as they offer new opportunities to fine tune the electronic and structural properties of gold nanoclusters. Following the discovery of the hollow gold cages, two recent theoretical studies that focused on doping the cages with a foreign atom have appeared. Because the parent  $\text{Au}_{16}^-$  and  $\text{Au}_{17}^-$  cluster anions are empty cages, many different types of atoms could be used as dopants to form new endohedral gold clusters. In this highlight, we report the first use of photoelectron spectroscopy (PES) analysis and density functional

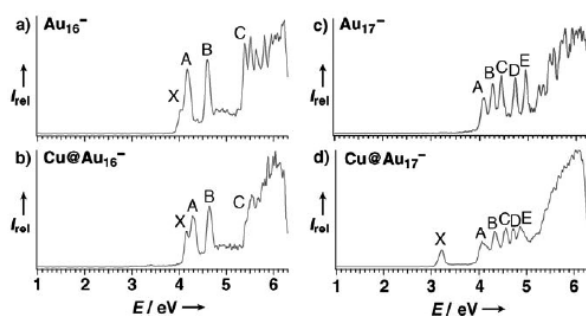
theory (DFT) calculations to observe and characterize  $\text{Au}_{16}^-$  and  $\text{Au}_{17}^-$  doped with a Cu atom ( $\text{Cu@Au}_{16}^-$  and  $\text{Cu@Au}_{17}^-$ ).

Figure 1 shows the spectra of  $\text{CuAu}_{16}^-$  and  $\text{CuAu}_{17}^-$  ions along with the of the parent gold clusters. First, we focus on the  $\text{CuAu}_{16}^-$  ion (Figure 1b), whose PE spectrum is remarkably similar to that of its parent gold cluster  $\text{Au}_{16}^-$  (Figure 1a). The similarity between the spectra of these two species suggests that Cu doping does not alter the geometric and electronic structures of the  $\text{Au}_{16}^-$  cluster anion significantly, which is only possible if the Cu is trapped inside the  $\text{Au}_{16}^-$  cage.

The spectrum of the doped cluster anion  $\text{CuAu}_{17}^-$  is also very similar to that of the parent gold cluster  $\text{Au}_{17}^-$ , except that there is one low-binding-energy peak followed by a large energy gap in the spectrum of the Cu-doped cluster (Figures 1c and d). This spectral similarity again suggests that the Cu dopant induces very little structural change in the  $\text{Au}_{17}^-$  cage except that it donates one electron.  $\text{Au}_{17}^-$  is a closed-shell species with 18 valence electrons; therefore, the extra electron is expected to enter its lowest occupied molecular orbital and give rise to the low-binding-energy peak (X) in the PE spectrum of the  $\text{CuAu}_{17}^-$  cluster anion (Figure 1d). All these observations again imply that Cu stays in the center of the  $\text{Au}_{17}^-$  ion cage ( $\text{Cu}^+@Au_{17}^{2-}$ ) and does not perturb the electronic and geometric structures of the cage significantly.

We carried out theoretical studies to confirm these observations. The results revealed that the endohedral  $\text{Cu@Au}_{16}^-$  and  $\text{Cu@Au}_{17}^-$  cluster anions are overwhelmingly favored over any other structure with the Cu atom on the outside of the cage. Figure 2 shows the simulated PE spectra for two endohedral structures each for the  $\text{Cu@Au}_{16}^-$  and  $\text{Cu@Au}_{17}^-$  cluster anions along with those of the parent clusters. In one structure, the Cu atom is located in the center of the cages, and in the other structure, it is displaced slightly from the center. The energy differences between the two isomers are very small, and their simulated PE spectra are also very similar to each other. The calculated vertical detachment energies for the  $\text{Cu@Au}_{16}^-$  and  $\text{Cu@Au}_{17}^-$  cluster anions also are in good agreement with the experimental values. Overall, the excellent agreement between theory and experiment unequivocally confirms the endohedral structures of these Cu-doped gold cages.

Doping gold clusters could be a powerful way to tune their chemical and physical properties, and the results reported in this highlight suggest that a new class of endohedral gold cages is indeed viable. In these examples, the cage structures of  $\text{Au}_{16}^-$  and  $\text{Au}_{17}^-$  cluster anions are maintained simply by changing the dopants, which is reminiscent of the behavior of endohedral fullerenes. It would be particularly interesting to dope transition-metal atoms inside these gold cages to create magnetic gold clusters as the resulting material may exhibit new, physical, chemical, and catalytic properties that are distinct from the pure gold clusters.



**Figure 1.** Photoelectron spectra of the cluster anions  $\text{CuAu}_{16}^-$  and  $\text{CuAu}_{17}^-$  (Figures 1b and 1d), compared to the parent gold clusters  $\text{Au}_{16}^-$  and  $\text{Au}_{17}^-$  (Figures 1a and 1c).

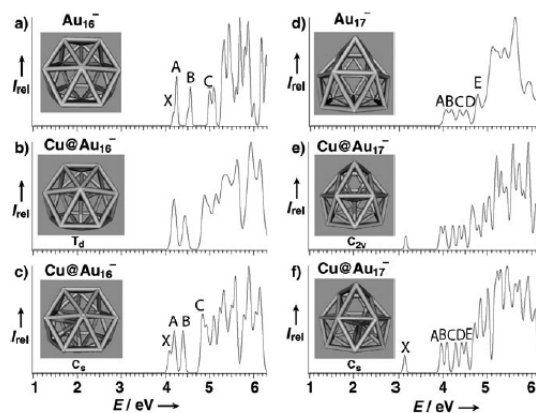


**Figure 2.** Simulated photoelectron spectra for two endohedral structures each for  $\text{Cu@Au}_{16}^-$  and  $\text{Cu@Au}_{17}^-$  along with those for  $\text{Au}_{16}^-$  and  $\text{Au}_{17}^-$ .

This exciting work was published online in the April 13, 2007, edition of the journal *Angewandte Chemie* (Wang et al. 2007).

#### Citation

Wang LM, S Bulusu, HJ Zhai, XC Zeng, and LS Wang. 2007. "Doping Golden Buckyballs: Cu@Au<sub>16</sub><sup>-</sup> and Cu@Au<sub>17</sub><sup>-</sup> Cluster Anions." *Angewandte Chemie* 46(16):2915-2918.

## Solid-State NMR Characterization of CdS Nanoparticle/Polymer Interfaces

**MP Espe,<sup>(a)</sup> S Ortiz,<sup>(a)</sup> and SD Burton<sup>(b)</sup>**

**(a) University of Akron, Akron, Ohio**

**(b) W.R. Wiley Environmental Molecular Sciences Laboratory, Richland, Washington.**

*Semiconducting nanoparticles made from cadmium chalcogenide have unique optical, catalytic and energy transfer properties stemming from their size and morphology. To better understand the physical properties created during the processing of these nanopartical materials, nuclear magnetic resonance (NMR) spectrometry is one of the tools used to investigate atomic structure and substrate-surface interactions.*

Cadmium chalcogenide (CdX; X = S, Se, Te) semiconducting (II-VI) nanoparticles are currently of significant interest because the properties of the nanoparticles are intermediate to those of molecular and bulk materials, which have a diverse number of realized and potential applications. Several of these applications include organic/inorganic light-emitting diodes, electroluminescence devices, nanoelectronics, quantum-dot LASERs, photovoltaic solar cells, catalysts, materials for imaging, and assaying bio-systems. In most of these systems, the critical property of the nanoparticle is its photoluminescence, for which the emission wavelength can be varied by varying the particle size. The photoluminescent properties are highly dependent on the surface structure of the nanoparticle, with high defect numbers producing more trapped-state luminescence. The surface defect sites can be electronically passivated by coating the CdX nanoparticle surfaces with capping agents, such as phosphine oxides, thiols, and amines. These passivated particles luminesce predominantly through band-edge emissions, resulting in longer excitation lifetimes and higher luminescent intensities.

Solid-state NMR is the ideal technique for the study of the structure of CdX nanomaterials as both the bulk and surface structures of the NMR active nuclei can be probed. In addition, the interaction between the nanoparticles and the surface passivation materials can be characterized. NMR studies of the CdX materials benefit from the presence of an array of ideal NMR active nuclei, including <sup>113</sup>Cd (12.26 percent natural abundance [n.a.], spin=1/2), <sup>77</sup>Se (7.6 percent n.a., spin=1/2), <sup>125</sup>Te (7 percent n.a., spin=1/2), and <sup>13</sup>C (1.1 percent n.a., spin=1/2).

The materials analyzed using capabilities in the EMSL High Field Magnetic Resonance Facility were cadmium sulfide (CdS) nanoparticles synthesized using two different capping agents: 1-thioglycerol and 4-bromophenylethenyl phosphonic acid (4BrEPPA). In summary, the cadmium chemical shift shows the successful formation of cadmium nanoparticles resulting from the resultant chemical shift and a wide line caused by structural heterogeneity. The lower spectrum shown in Figure 1 represents all the cadmium present in the sample, while the top spectrum of these represents that cadmium at the surface of the nanoparticles. The spectral editing was generated using a H-Cd cross polarization magic-angle spinning technique that uses protons on the surface to enhance the surface cadmium signal. There is a small fraction of cadmium at the surface compared to the whole sample.

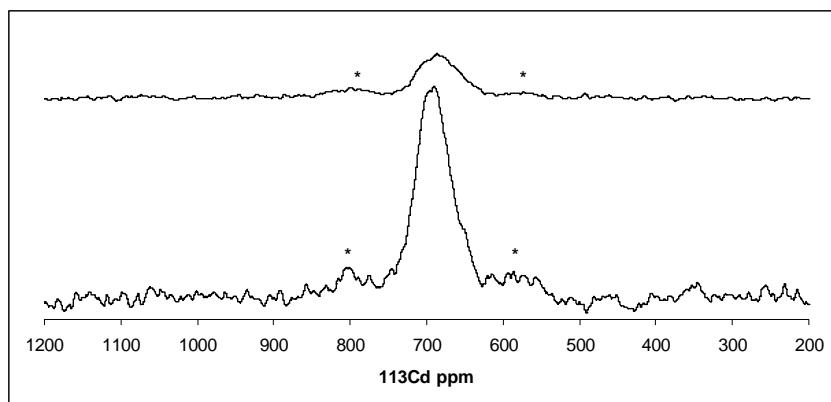


**Figure 1.** Parts per million (ppm)  $^{113}\text{Cd}$  of CdS as synthesized, DP (bottom,  $d1=60$  sec,  $ct=1146$ ,  $lb=200$ ,  $ss$  5 KHz) and CP (top,  $d1=2$ sec,  $cp=1$ ms,  $ct=13660$ ,  $lb=200$ ,  $ss$  5 KHz)

A two-dimensional heteronuclear correlation experiment was performed on the CdS precipitated with ethanol. In that experiment, the correlation between the protons (F1 dimension) and the cadmium (F2 dimension) in the sample was observed (see Figure 2). The two protons were observed to have a strong correlation with the cadmium of the CdS nanoparticles, one at approximately 4 ppm representing correlation with protons of  $\text{CH}_2$  close to the sulfur and the CH and the other at about 8 ppm, possibly resulting from protons of the OH groups at the surface of the CdS.

These and additional results, which discussed synthesis, further analysis, and the effects of hydration on the surface, were presented July 22, 2008, at the NMR Symposium during the Rocky Mountain Analytical Conference, in Breckenridge Colorado.

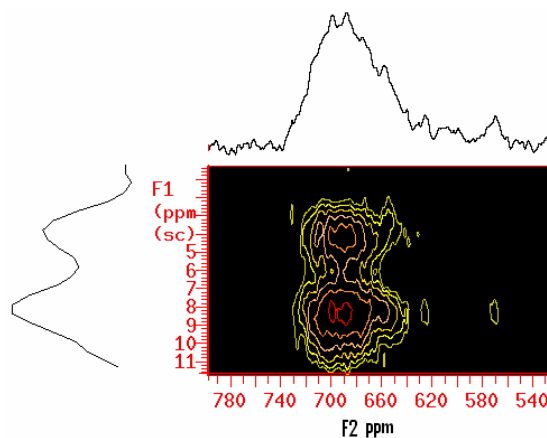


**Figure 2.**  $^1\text{H}$ - $^{113}\text{Cd}$  heteronuclear correlation experiment on CdS precipitated with ethanol.

## Bio-Stimulation of Iron Reduction and Subsequent Oxidation of Sediment Containing Fe-Silicates and Fe-Oxides: Effects of Redox Cycling on Fe(III) Bio-Reduction

J Komlos,<sup>(a)</sup> RK Kukkadapu,<sup>(b)</sup> JM Zachara,<sup>(c)</sup> and PR Jaffé<sup>(a)</sup>

(a) Princeton University, Princeton, New Jersey

(b) W.R. Wiley Environmental Molecular Sciences Laboratory, Richland, Washington

(c) Pacific Northwest National Laboratory, Richland, Washington

*Effective bio-remediation depends on the durability of bio-reduced sediments to trap contaminants. This study determined that iron silicates in sediments can be repeatedly bio-reduced and re-oxidized, thus forming a cyclical means of sequestering contaminants in the environment.*

Sediment containing a mixture of iron(Fe)-phases, including Fe-oxides and Fe-silicates, was bio-reduced in a long-term flow-through column experiment followed by re-oxidation with dissolved oxygen. This study determined the nature of the re-oxidized Fe(III) and how redox cycling of Fe would affect subsequent Fe(III) bio-availability. In addition, the effect of manganese (Mn) on Fe(III) reduction was explored. <sup>57</sup>Fe-Mössbauer spectroscopy measurements showed that bio-stimulation resulted in partial reduction (20 percent) of silicate Fe(III) to silicate Fe(II), while the reduction of Fe-oxides was negligible. Furthermore, the reduction of Fe in the sediment was uniform throughout the column, suggesting that Fe is not mobilized. As shown in Figure 1, the Mössbauer spectra of the re-oxidized sample were similar to that of pristine sediment implying that Fe-mineralogy of the re-oxidized sediment was mineralogically similar to that of the pristine sediment. Batch experiments showed that Fe(III) reduction occurred at a similar rate although the time required for Fe(II) accumulation to begin was longer in the pristine sediment than the re-oxidized sediment under identical seeding conditions. This rate change was attributed to oxidized Mn that acted as a temporary redox buffer in the pristine sediment. The oxidized Mn was transformed to Mn(II) during bio-reduction but, unlike silicate Fe(II), the Mn(II) was not re-oxidized when exposed to oxygen. A paper describing the results of this research was published in the July 2007 edition of the journal *Water Research* (Komlos et al. 2007).

### Citation

Komlos J, RK Kukkadapu, JM Zachara, and PR Jaffé. 2007. "Biostimulation of Iron Reduction and Subsequent Oxidation of Sediment Containing Fe-Silicates and Fe-Oxides: Effect of Redox Cycling of Fe(III) Bioreduction." *Water Research* 41(13):2996-3004.

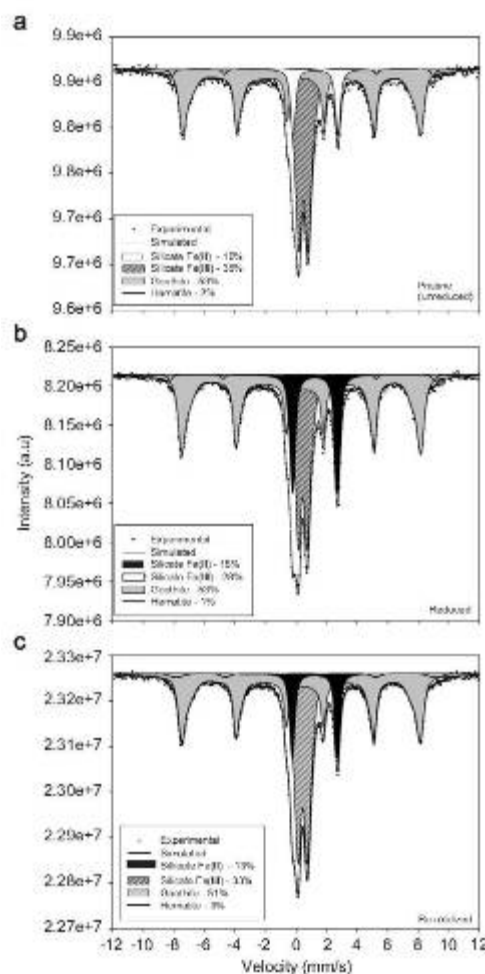


**Figure 1.** Mössbauer spectra (12K) of the (a) pristine sediment, (b) bio-reduced sediment, and (c) re-oxidized sediment.

## Probing Oxidative Stress Using Intact-Protein, High-Field LC-FTICR Mass Spectrometry

NM Lourette,<sup>(a)</sup> HS Smallwood,<sup>(a)</sup> CB Boschek,<sup>(a)</sup> S Wu,<sup>(a)</sup> RD Smith,<sup>(a)</sup> TC Squier,<sup>(a)</sup> and L Paša-Tolić<sup>(a)</sup>

(a) Pacific Northwest National Laboratory, Richland, Washington

*Mechanisms that regulate the removal of nitrated and oxidized proteins in cells are critical for preventing a number of diseases (such as diabetes, cardiovascular disease, cancer, and neurological disorders), as well as for reducing the effects of aging. In this work, we used high-resolution liquid chromatography (LC) separations in conjunction with high-mass-measurement accuracy and high-resolution measurements afforded by 12 tesla Fourier transform ion cyclotron resonance (FTICR) mass spectrometer in the EMSL High-Performance Mass Spectrometry Facility to probe oxidative stress in calmodulin, which is a signaling protein in macrophages. Importantly, we identified a novel oxidation-dependent lysine cleavage that potentially acts as a biomarker of oxidative stress.*

Oxidative species not only mediate static and tidal effects on a variety of pathogens, but also nitrate and oxidize host proteins during the immune response. These post-translational modifications (PTMs) to intracellular proteins in various inflammatory states also are implicated in many age-related diseases. In this context, the accumulation of nitrotyrosines in proteins may result from an aberrant repair pathway. Previous works have postulated denitrase activity in various tissues based on the loss of immunoreactivity involving antibodies against nitrotyrosine. However, attributing the loss in immunoreactivity to denitration is equivocal, as this effect may be caused by degradation of the nitrated protein, alterations in protein structure that cover the epitope, chemical alteration of the nitrotyrosine, and/or enzymatic denitration.

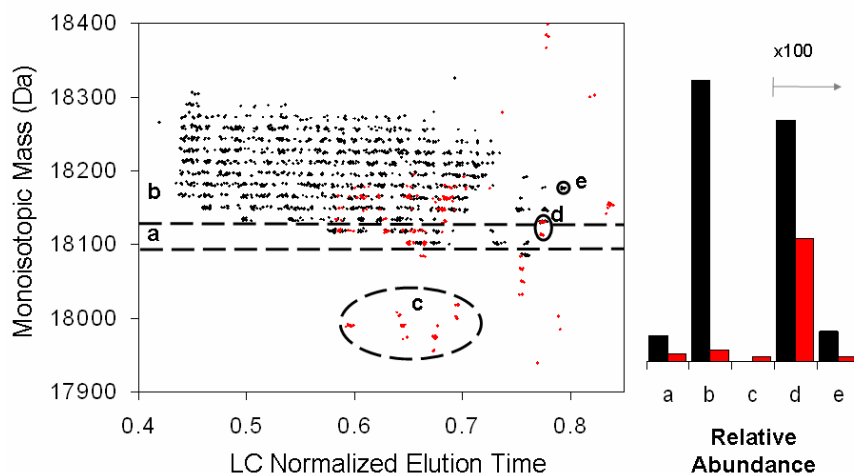


**Figure 1.** The time vs. mass two-dimensional display (left) highlights our ability to resolve intact protein masses of individual oxidized CaM species that are indicators of denitrase activity. CaM species detected prior to (red symbols) and following (black symbols) incubation with cell lysate from activated macrophages: a) CaM & CaMox; b) nYCaMox & 2nYCaMox; c) CaM-Lysine and CaMox-Lysine; d) nYCaM, and e) 2nYCaM. The panel at the right displays the relative abundance of CaM within each of these five areas. Definitions of the abbreviations follow: CaM, calmodulin; CaMox (nYCaMox), oxidized CaM containing methionine sulfoxides or (and) nTyr.

Characterization of the product following denitration and corresponding loss of immunoreactivity requires the use of an analytical tool that can confirm the involvement of specific proteins, thereby ruling out the ambiguous interpretations based on antibody recognition.

We used intact protein reversed phase LC-FTICR mass spectrometry to monitor the time dependent changes in the nitration of calmodulin (nYCaM) in macrophages following macrophage activation with lipopolysaccharide endotoxin (Figure 1). Tentative identifications of PTMs were assigned by combining tryptic peptide information generated from bottom-up analyses with online collision-induced dissociation tandem mass spectrometry at the intact protein level, which confirmed localization of the nitrated sites. Our results indicate that macrophage activation associated with an oxidative burst stimulates a dramatic reduction in the abundance and diversity of oxidatively modified proteins. More specifically, we established that macrophage repair pathways can repair nitrated tyrosines and oxidized methionines within a signaling protein (i.e., calmodulin) to their original unmodified states to retain optimal protein function.

We also identified a modification dependent C-terminal lysine cleavage that is likely to alter calmodulin function. We propose that the cleaved calmodulin is a useful biomarker of intracellular oxidative stress conditions because of both the oxidation dependence of this lysine cleavage and the stability of the cleavage product. This stability is in contrast to the reversible modifications we observed for nitrotyrosine and methionine sulfoxide. The transient nature of nitrotyrosine and methionine sulfoxide renders these currently used biomarkers as inaccurate. Portions of this work have been detailed in a manuscript accepted for publication in the journal *Biochemistry*.

## Oriented ZnO Films Deposited by MOCVD with Low Carbon Concentrations

LV Saraf,<sup>(a)</sup> MH Engelhard,<sup>(a)</sup> CM Wang,<sup>(a)</sup> AS Lea,<sup>(a)</sup> DE McCready,<sup>(a)</sup>  
V Shutthanandan,<sup>(a)</sup> DR Baer,<sup>(a)</sup> and SA Chambers<sup>(b)</sup>

(a) W.R. Wiley Environmental Molecular Sciences Laboratory, Richland, Washington

(b) Pacific Northwest National Laboratory, Richland, Washington

*Growth of high-purity and carbon-free, wide-band-gap semiconductors is very important for researchers in the optical and semiconductor industries. Carbon contamination is one of the major problems in metal organic chemical vapor deposition (MOCVD) semiconductor growths because the majority of the precursors are carbon dominated. In this report, we show that successful decomposition of Zn(TMHD)2 precursor resulted in low-carbon ZnO films.*

The use of environmentally friendly precursors in the MOCVD process is essential because of safety hazards present in commonly used precursors. Because of the popularity and usefulness of ZnO material in transparent conducting oxide coating, spintronics, catalysis, and sensors, literature on ZnO growth by MOCVD is plentiful. Most of the work is based on use of hazardous di-methyl zinc (DMZ), di-ethyl zinc (DEZ), zinc acetate, zinc acetylacetonate-based precursors. In this report, we discuss the relatively uninvestigated Zn(TMHD) precursor for the growth of oriented ZnO films on silicon. The cleanliness of the Zn(TMHD) precursor decomposition was determined by measuring the amount of carbon in the deposited films. We show by x-ray photoelectron spectroscopy (XPS) that despite the high carbon content in the precursor (i.e., C22 in a single Zn(TMHD)2 precursor molecule), much less than 1 atomic (at.) % carbon was present in ZnO films grown with this precursor.

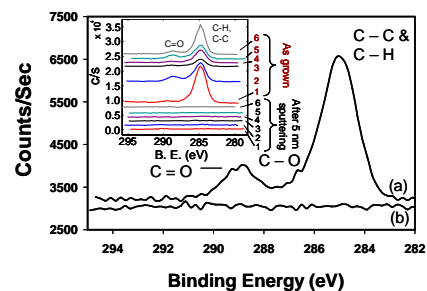


**Figure 1.** High-resolution C 1s spectra of ZnO films before and after sputtering.

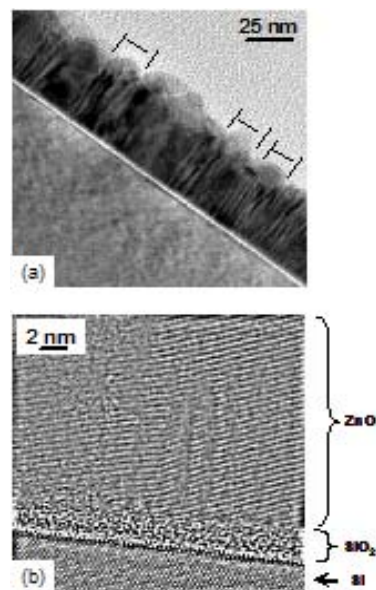


Figure 1 shows high resolution C 1s spectra before and after sputtering. The overall C concentration at the surface was 21 at. %, and was reduced after sputtering to below 1 at. %. Excess oxygen, revealed by an increase in the O to Zn ratio, is attributed to the presence of C-O and C=O functionalities on the surface. Removal of surface C layer appeared to restore the Zn/O ratio to 1:1. The inset in Figure 1 represents the reproducibility of our results. These spectra indicate high-resolution XPS scans of C 1s for ZnO films grown on single crystal silicon and Al<sub>2</sub>O<sub>3</sub>. The two sets of spectra represent carbon content on as-grown ZnO surfaces before and after 5 nm sputtering of the same position. Sample numbers 1, 3, and 4 are grown on single-crystal silicon, samples 2 and 6 on single-crystal c-plane Al<sub>2</sub>O<sub>3</sub>, and sample number 5 on r-plane Al<sub>2</sub>O<sub>3</sub> under similar conditions.

As expected, we have not detected any substrate relationship to carbon content. The surface carbon concentration in the as-grown films was observed to be in the range of 11 to 34 at. %. However, the carbon was reduced to much less than 1 at. % on all samples after 5 nm of sputtering. Figure 2 indicates low- and high-resolution transmission electron microscope (TEM) micrographs of a typical ZnO film grown on silicon. A columnar structure in low-resolution TEM and the c-axis oriented atomic planar arrangement of ZnO are clearly visible in the images. A paper describing this research was published in the May issue of the *Journal of Materials Research* (Saraf et al. 2007).

#### Citation

Saraf LV, MH Engelhard, CM Wang, AS Lea, DE McCready, V Shutthanandan, DR Baer, and SA Chambers. 2007. "Metalorganic Chemical Vapor Deposition of Carbon-Free ZnO Using the Bis(2,2,6,6-tetramethyl-3,5-heptanedionato) Zinc Precursor." *Journal of Materials Research* 22(5):1230-1234.



**Figure 2.** Low- and high-resolution TEM images of ZnO films.

## Nucleation and Growth of MOCVD Grown (Cr, Zn)O Films: Uniform Doping vs. Secondary Phase Formation

LV Saraf,<sup>(a)</sup> MH Engelhard,<sup>(a)</sup> P Nachimuthu,<sup>(a)</sup> V Shutthanandan,<sup>(a)</sup> CM Wang,<sup>(a)</sup>  
SM Heald,<sup>(a)</sup> DE McCready,<sup>(a)</sup> AS Lea,<sup>(a)</sup> DR Baer,<sup>(a)</sup> and SA Chambers<sup>(b)</sup>

(a) W.R. Environmental Molecular Sciences Laboratory, Richland, Washington

(b) Pacific Northwest National Laboratory, Richland Washington

*Understanding of doping limitations in wide-band-gap semiconductors is crucial before using them for various studies. Zinc oxide (ZnO) is a popular wide-band-gap semiconductor (oxide) studied for its usefulness in light emission, transparency, and doping-assisted, band-gap tuning ability. In this report, we focus on major limitations for chromium as a dopant in ZnO resulting secondary phase formations.*

ZnO is a II-VI semiconducting oxide with the bandgap of 3.3 eV. It stabilizes in the hexagonal structure with lattice constants 0.32 nm (a) and 0.52 nm (c). ZnO is a well-known, multi-functional oxide that is useful in thermoelectric, optical, magnetic, dielectric, and sensing applications. Chromium (Cr) is of potential interest as a magnetic and electronic dopant in ZnO. Thus, the aim of this study was to determine the extent to which Cr can be incorporated into the ZnO lattice as a substitutional cation. From our results, we concluded that little, if any, Cr occupies tetrahedral sites in the ZnO lattice. Instead, the secondary phases and  $\text{ZnCr}_2\text{O}_4$ , in which Cr is in octahedral sites, preferentially nucleate.  $\text{Cr}_2\text{O}_3$  is present predominantly as a disordered phase at the interface.  $\text{ZnCr}_2\text{O}_4$  also is largely segregated at the interface, although some nanocrystalline  $\text{ZnCr}_2\text{O}_4$  may be present in the ZnO matrix.

Figure 1 indicates particle induced x-ray emission (PIXE) results for ZnO and (Cr, Zn)O films. The experimental PIXE data are shown as solid circles and the solid curve represents K-fitted spectra for pure and (Cr, Zn)O films. The initial peak at 0.7 is from  $\text{K}\beta$  lines. Peaks representing Cr lines are clearly seen in Figure 1b. The total Cr atomic percentage (at. %) in the film is 5.5 at. %. However, from an x-ray photoelectron spectroscopy depth profile and Rutherford backscattering measurements as shown in Figure 2, very little chromium is observed at the surface. As seen in Figures 1 and 2, a good correlation is observed between the two profiles (i.e., evidence of Cr-rich interface is visible). We have also confirmed from extended x-ray absorption fine structure measurements that Cr indeed occupies octahedral position. X-ray diffraction analysis also was performed to confirm the identity of the secondary spinel phases. The data discussed in this study clearly show that the solid solubility of Cr is significantly less in ZnO.

### Citation

Saraf LV, MH Engelhard, P Nachimuthu, V Shutthanandan, CM Wang, SM Heald, DE McCready, AS Lea, DR Baer, and

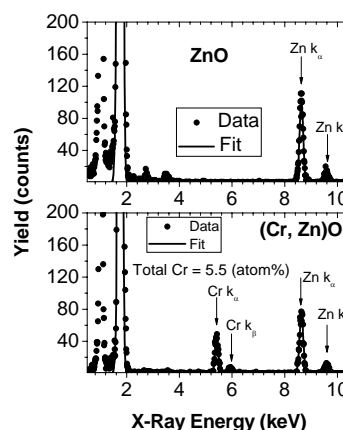


**Figure 1.** PIXE spectra of (a) pure ZnO and (b) (Cr, Zn)O films

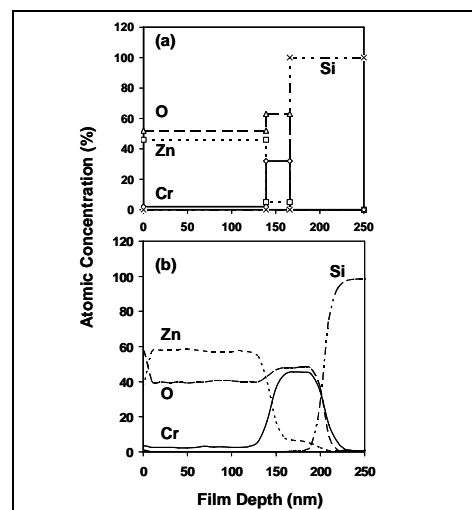


**Figure 2.** Rutherford backscattering and x-ray photoelectron spectroscopy depth profiles for (Cr, Zn)O films.

SA Chambers. 2007. "Nucleation and Growth of MOCVD Grown (Cr, Zn)O Films." *Journal of the Electrochemical Society* 154(3):D134-D138.

## Atomistic Simulations of Hydrated Nafion and Temperature Effects on Hydronium Ion Mobility

A Venkatnathan,<sup>(a)</sup> R Devanathan,<sup>(a)</sup> and M Dupuis<sup>(a)</sup>

(a) Pacific Northwest National Laboratory, Richland, Washington

*Polymer electrolyte membrane fuel cells (PEMFCs) can generate power with high efficiency and minimal greenhouse gas emissions. They have the potential to revolutionize power generation for the transportation, residential, and aerospace sectors. The polymer membrane is the heart of the fuel cell. Desired membrane properties are high proton conductivity; thermal, mechanical, and chemical stability; and low cost. None of the existing membranes meet all these requirements. There is a pressing need to design and optimize fuel cell membranes based on a molecular-level understanding of proton transport in polymer membranes.*

In this study, molecular simulations are employed to study nanostructure and molecular transport in the widely used polymer membrane, Nafion™ (Dupont). The results reveal that the extent of membrane hydration specifically affects the sulfonate groups on the polymer chains where protons tend to reside. Figure 1 shows a snapshot of a Nafion membrane at low hydration and radial distribution functions at various hydration levels.

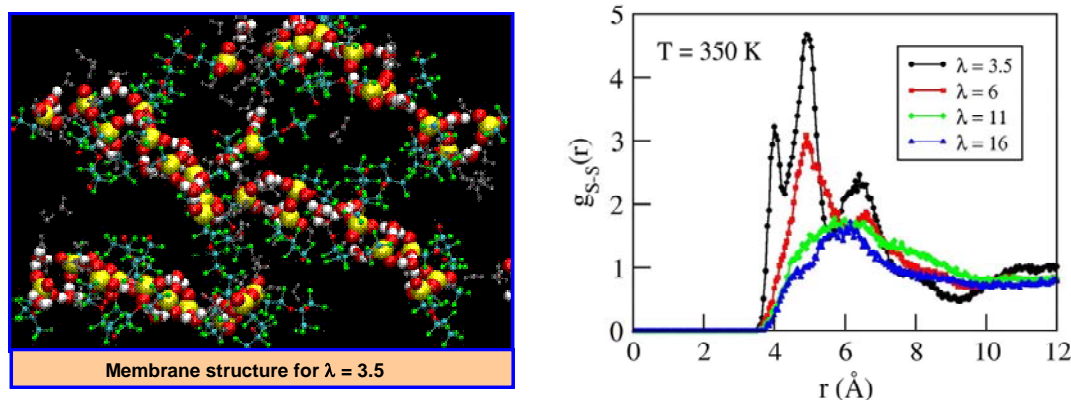


**Figure 1.** Left: Snapshot of hydrated Nafion membrane at low hydration. Right: Radial distribution functions of sulfur atoms in hydrated Nafion.

At low hydration levels of a Nafion membrane, the sulfonate groups aggregate, which diminishes proton transport through the membrane. At higher membrane hydration levels, the distance between the sulfonate groups increases, thereby enhancing proton transport. The dynamical properties of proton and water transport, such as diffusion at fuel cell operating temperatures, also have been examined. This work was recently published as a cover article in the *Journal of Physical Chemistry B* (Venkatnathan et al. 2007). More recently, a detailed examination of the nanostructure of Nafion and the dynamics of proton and water using a different force-field model was performed. The local structure of Nafion membrane around the acidic sulfonate groups that are critical for proton transport is shown in Figure 2. Details of this work appeared in the *Journal of Physical Chemistry B* (Devanathan et al. 2007). The results, which are in good agreement with experimental measurements of the water diffusion coefficient in hydrated Nafion, help in the interpretation of results obtained from recent neutron scattering experiments.

## Citations

Devanathan R, A Venkatnathan and M Dupuis. 2007. "Atomistic Simulation of Nafion Membrane: I. Effect of Hydration on Membrane Nanostructure." *Journal of Physical Chemistry B* 111(28):8069-8079.

Venkatnathan A, R Devanathan, and M Dupuis. 2007. "Nanostructure of Proton Exchange Membrane Under Low Hydration and Hydronium Mobility: Atomistic Simulation and Characterization." *Journal of Physical Chemistry B* 111(25):7234-7244.

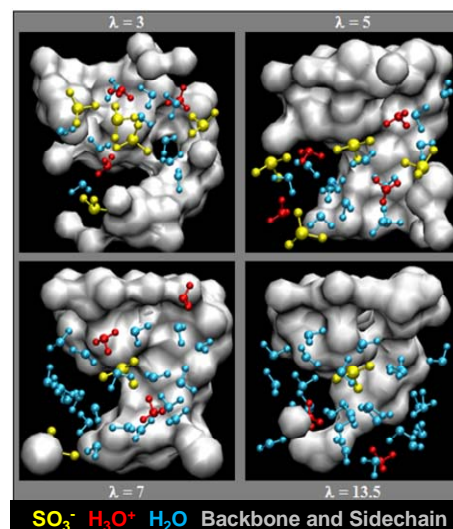


**Figure 2.** Snapshot of local structure of hydrated Nafion membrane at various level of membrane hydration ( $\lambda$ ).

## Scientific Grand Challenge Highlights

### Systems Approach to Understanding the Molecular Mechanism of the Light-Dark Cycles of *Cyanothece* sp. 51142

**C Oehmen,<sup>(a)</sup> J McDermott,<sup>(a)</sup> J Stockel,<sup>(b)</sup> E Welsh,<sup>(b)</sup> J Jacobs,<sup>(a)</sup> T Metz,<sup>(a)</sup> A Dohnalkova,<sup>(c)</sup> GW Buchko,<sup>(a)</sup> and HB Pakrasi<sup>(b)</sup>**

**(a) Pacific Northwest National Laboratory, Richland Washington**

**(b) Washington University, St. Louis St. Louis, Missouri**

**(c) W.R. Wiley Environmental Molecular Sciences Laboratory, Richland, Washington**

*Studying complex biological phenomena at multi-levels of detail requires analyzing different types of data from many sources, including imaging technologies, bio-informatics, transcriptomics, and proteomics. As a wider variety of high throughput methods enter mainstream scientific analyses, handling the complexity and volume of data from these disparate sources requires new algorithms for processing, visualization, and analysis.*

We present integrative, multi-level analysis of circadian cycling in *Cyanothece* sp. 51142 under the auspices of the EMSL Grand Challenge in Membrane Biology project, which is a multi-institutional collaboration among Washington University in St. Louis, Purdue University, Saint Louis University, the Danforth Center in St. Louis, and PNNL. The focus of the Grand Challenge consortium is to understand how cycling of metabolites, gene expression, and proteins leads to physiological changes in *Cyanothece* during light and dark cycles. Integration of correlations across transcriptomic, proteomic, and metabolomic datasets is being accomplished with a novel suite of computational tools developed at PNNL. These integrated tools include Similarity Box (Sofia and Nakamura 2007), an interactive dendrogram/clustering tool, PQuad (Harve et al. 2004), a proteomics dataset viewer, SEBINI (Taylor et al. 2006), a network inference environment and

ScalaBLAST (Oehmen and Nieplocha 2006), and a high-performance BLAST accelerator (Altschul et al. 1990). Analyzing this large and complex collection of datasets using novel tools and hardware has made it possible to identify vital molecular components in the circadian cycles. Once identified, the goal is to experimentally verify the importance of these components *in vivo*.

### Citations

Sofia HJ and GC Nakamura. 2007. “Similarity Box: Visual Analytics for Large Genomic Sets.” (submitted to *Bioinformatics*).

Havre SL, M Singhal, DA Payne, and BM Webb-Robertson. 2004. “PQuad: Visualization of Predicted Peptides and Proteins.” *Visualization, 2004, IEEE* 473-480.

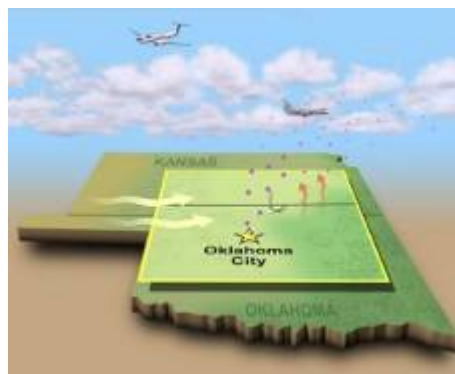
Taylor RC, A Shah, CC Treatman, and ML Blevins. 2006. “SEBINI Software Environment for Biological Network Inference.” *Bioinformatics* 22(21):2706-2708.

Oehmen CS and J Nieplocha. 2006. “ScalaBLAST: A Scalable implementation of BLAST for high-performance data-intensive bioinformatics analysis” *IEEE Transactions on Parallel and Distributed Systems* 17(8):740-749.

Altschul SF, W Gish, W Miller, EW Myers, and DJ Lipman. 1990. “Basic Local Alignment Search Tool.” *Journal of Molecular Biology* 215(3):403-410.

## Awards and Recognition

**EMSL expertise and instrumentation used to support the Cumulus Humilis Aerosol Processing Study.** EMSL staff members ML Alexander, Y Dessiaterik, A Laskin, and M Newburn and users CM Berkowitz and LK Berg are supporting an atmospheric field campaign in Oklahoma that seeks a better understanding of how aerosols affect cloud properties such as water concentration and droplet size distributions. The campaign also is studying how clouds affect properties of aerosols like chemical composition and location in the atmosphere. EMSL’s proton reaction transfer mass spectrometer was deployed in the Battelle Gulfstream-1 research aircraft to measure aerosol composition and related chemistry. Data obtained from these measurements, along with measurements about the state of the atmosphere, will be compared with new algorithms that represent cloud and aerosol processes in climate models. The campaign allows researchers to obtain a focused data set during a key seasonal period in the region—winter wheat harvest—that coincides with fair weather clouds (cumulus humilis) throughout the Midwest. The campaign involves multiple agencies from across the nation and was conducted in conjunction with the Cloud and Land Surface Interaction Campaign, led by Brookhaven National Laboratory, which is investigating how changes in land use affect clouds through changes to surface heating and associated dynamics. The Cumulus Humilis Aerosol Processing Study (CHAPS) is supported by the U.S. Department of Energy’s Atmospheric Science Program under the Office of



The primary goal of the CHAPS campaign is to characterize and contrast freshly emitted aerosols above, within, and below fields of cumulus humilis (or fair-weather cumulus) clouds. These observations will be used to examine the aerosol optical properties and cloud nucleating properties from both below and above clouds, and how they differ downwind of a mid-size city relative to similar aerosols in air less affected by emissions.



Biological and Environmental Research.

**EMSL staff member receives President's Volunteer Service Award.** EMSL researcher KM Beck is the first Battelle staff member to receive the President's Volunteer Service Award. This award, an initiative of the President's Council on Service and Civic Participation, honors America's volunteers and encourages even more Americans to get involved in volunteer activities. Beck served more than 250 hours with the U.S. Coast Guard Auxiliary District 13 and the Black Rock City Emergency Services Department over the last year. That number of hours earned him a Silver Award from the President's Volunteer Service Award program. He was honored June 26, 2007, at the Volunteer Appreciation and Community Service Award reception held in the Battelle Auditorium.



Mike Kluse, Acting PNNL Director, with KM Beck, recipient of the President's Volunteer Service Award.

**EMSL staff graduate from scientist and engineer program.** N Jaitly and BL LaMarche of the EMSL Instrument Development Laboratory graduated from PNNL's Scientist and Engineer Development Program in June after successful completion of the two-year professional skills mentoring program.

## Professional/Community Service

**Collaborations with Appalachian State University.** Scientists from Appalachian State University in Boone, North Carolina, collaborated with a PNNL researcher to vet various theoretical models against careful analytical work to determine which programs could best model experimental data for a method useful not only to basic science, but also to real-world applications such as environmental monitoring/restoration. The accuracy of various computational methods (Hartree-Fock, MP2, CCSD, CAS-SCF, and several types of Density Functional Theory) for predicting relative intensities in Raman spectra for  $C_6H_6$ ,  $C_6D_6$ , and  $C_6F_6$  was compared. The predicted relative intensities for  $\nu_1$  and  $\nu_2$  were compared with relative intensities measured by a Fourier Transform-Raman spectrometer. While none of these methods were found to excel at this prediction, Hartree-Fock with a large basis set was most successful for  $C_6H_6$  and  $C_6D_6$ , while PW91PW91 was the most successful for  $C_6F_6$ . Results were reported in the journal *Theoretical Chemistry Accounts* (Williams et al. 2007). The research team included EMSL users S Williams, T Gibbons, and C Kitchens (Appalachian State University) and T Johnson (PNNL). Computer time was supported by collaborative high-performance computing resources funding through the Office of the President of the University of North Carolina.

### Citation

Williams SD, TJ Johnson, TP Gibbons, and CL Kitchens. 2007. "Relative Raman Intensities in  $C_6H_6$ ,  $C_6D_6$ , and  $C_6F_6$ : A Comparison of Different Computational Methods." *Theoretical Chemistry Accounts* 117(2):283-290.

**EMSL researcher presents on EMSL-developed software tools.** N Jaitly of EMSL's Instrument Development Laboratory presented a tutorial at the U.S. Chapter of Human Proteome Organization's Conference in Seattle on the use of software tools developed at the Instrument Development Laboratory.

## Major Facility Upgrades

**Proteomic Analysis Capabilities Upgraded.** A new ThermoFisher LTQ-Oribitrap instrument was installed in EMSL in July 2007. This instrument is now fully functional and is providing much needed additional throughput for analysis of proteomic samples. Among instruments available for this kind of analysis, the LTQ-Oribitrap provides the best sensitivity, mass accuracy, and mass resolution available, all of which are critical analytical measures for achieving success in the field of proteomic research. Funding for this instrument was provided by a National Institutes of General Medical Sciences (NIGMS) Glue Grant titled, “Inflammation and the Host Response to Injury.” The NIGMS is a division of the National Institutes for Health. This collaborative program aims to uncover the biological reasons why patients can have dramatically different outcomes after suffering a traumatic injury. It is the first large-scale interdisciplinary program undertaken to attempt to solve the life-threatening problem of inflammation following major trauma or burn injury. Inflammation and the Host Response to Injury brings together major medical and research institutions with researchers in the fields of surgery, genomics, proteomics, biostatistics, bioinformatics, computational biology, and genetics to focus on the molecular biology of inflammation. More information can be found at <http://www.gluegrant.org/>.

## Visitors and Users

During this reporting period, a total of 341 users benefited from EMSL capabilities and expertise. This total included 245 onsite users and 96 remote users.

## New EMSL Staff

M Plumb joined EMSL in June as the new Administrator for the EMSL Magnetic Resonance and Mass Spectrometry Group. She has over 16 months of work experience at PNNL.

## Publications

Alexeev Y, MW Schmidt, TL Windus, and MS Gordon. 2007. “A Parallel Distributed Data CPHF Algorithm for Analytic Hessians.” *Journal of Computational Chemistry* 28(10):1685-1694.

Bondarchuk O, Y Kim, JM White, J Kim, BD Kay, and Z Dohnalek. 2007. “Surface Chemistry of 2-Propanol on TiO<sub>2</sub>(110): Low- and High-Temperature Dehydration, Isotope Effects, and Influence of Local Surface Structure.” *Journal of Physical Chemistry C* 111(29):11059-11067.

Buchko GW, S Ni, NM Lourette, R Reeves, and MA Kennedy. 2007. “NMR Resonance Assignments of the Human High Mobility Group Protein HMGA1.” *Journal of Biomolecular NMR* 38(2):185.

Cader T, LJ Westra, A Marquez, HJ McCallister, and KM Regimbal. 2007. “Performance of a Rack of Liquid-Cooled Servers.” *ASHRAE Transactions* 117(1):101-114.

Cao H, Y Xiong, T Wang, B Chen, TC Squier, and MU Mayer. 2007. “A Red Cy3-Based Biarsenical Fluorescent Probe Targeted to a Complementary Binding Peptide.” *Journal of the American Chemical Society* 129(28):8672-73,

Chambers SA, DA Schwartz, WK Liu, KR Kittilstved, and DR Gamelin. 2007. “Growth, Electronic and Magnetic Properties of Doped ZnO Epitaxial and Nanocrystalline Films.” *Applied Physics A, Materials Science and Processing* 88(1):1-5.

- Devanathan R, A Venkatnathan, and M Dupuis. 2007. "Atomistic Simulation of Nafion Membrane: I. Effect of Hydration on Membrane Nanostructure." *Journal of Physical Chemistry B* 111(28):8069-8079.
- Fang J, Z Gu, D Gang, C Liu, ES Ilton, and B Deng. 2007. "Cr(VI) Removal from Aqueous Solution by Activated Carbon Coated with Quaternized Poly(4-vinylpyridine)." *Environmental Science and Technology* 41(13):4748-4753.
- Farber R. 2007. "Keeping 'Performance' in HPC." *Scientific Computing* 24(8):15.
- Farber R. 2007. "The Cure for HPC Neurosis: Multiple, Virtual Personalities!" *Scientific Computing* 24(7):16.
- Feaver A, S Sepehri, P Shamberger, A Stowe, T Autrey, and G Cao. 2007. "Coherent Carbon Cryogel-Ammonia Borane Nanocomposites for H<sub>2</sub> Storage." *Journal of Physical Chemistry B* 111(26):7469-7472.
- Fu Y, J Laskin, and LS Wang. 2007. "Electronic Structure and Fragmentation Properties of [Fe<sub>4</sub>S<sub>4</sub>(SEt)<sup>4+</sup><sub>x</sub>(SSEt)<sub>x</sub>]<sup>2-</sup>." *International Journal of Mass Spectrometry* 263(2-3):260-266.
- Gu X, S Bulusu, X Li, XC Zeng, J Li, XG Gong, and LS Wang. 2007. "Au<sub>34</sub><sup>-</sup>: A Fluxional Core-Shell Cluster." *Journal of Physical Chemistry C* 111(23):8228-8232.
- Hammond JR, M Valiev, WA deJong, and K Kowalski. 2007. "Calculations of Molecular Properties in Hybrid Coupled-Cluster and Molecular Mechanics Approach." *Journal of Physical Chemistry A* 111(25):5492-5498.
- Hays J, KM Reddy, NY Graces, MH Engelhard, V Shutthanandan, M Luo, C Xu, NC Giles, C Wang, S Thevuthasan, and A Punnoose. 2007. "Effect of Co Doping on the Structural, Optical and Magnetic Properties of ZnO Nanoparticles." *Journal of Physics: Condensed Matter* 19(26): Art. No. 266203.
- Komlos J, RK Kukkadapu, JM Zachara, and PR Jaffé. 2007. "Biostimulation of Iron Reduction and Subsequent Oxidation of Sediment Containing Fe-Silicates and Fe-Oxides: Effect of Redox Cycling on Fe(III) Bioreduction." *Water Research* 41(13):2996-3004.
- Li XS, GE Fryxell, MH Engelhard, and C Wang. 2007. "The Synthesis of Cadmium Doped Mesoporous TiO<sub>2</sub>." *Inorganic Chemistry Communications* 10(6):639-641.
- Lin Y, G Liu, CM Wai, and Y Lin. 2007. "Magnetic Beads-based Bioelectrochemical Immunoassay of Polycyclic Aromatic Hydrocarbons." *Electrochemistry Communications* 9(7):1547-1552.
- Liu C, B Jeon, JM Zachara, and Z Wang. 2007. "Influence of Calcium on Microbial Reduction of Solid Phase Uranium(VI)." *Biotechnology and Bioengineering* 97(6):1415-1422.
- Liu G, H Wu, A Dohnalkova, and Y Lin. 2007. "Apoferitin-Templated Synthesis of Encoded Metallic Phosphate Nanoparticle Tags." *Analytical Chemistry* 79(15):5614-5619. DOI:10.1021/ac070086f
- Lower BH, L Shi, R Yongsunthon, TC Droubay, DE McCready, and SK Lower. 2007. "Specific Bonds between an Iron Oxide Surface and Outer Membrane Cytochromes MtrC and OmcA from *Shewanella oneidensis* MR-1." *Journal of Bacteriology* 189(13):4944-4952.
- McFarlane SA, JH Mather, and TP Ackerman. 2007. "Analysis of Tropical Radiative Heating Profiles: A Comparison of Models and Observations." *Journal of Geophysical Research. D. (Atmospheres)* 112(D14):D14218.



- Metz T, Q Zhang, JS Page, Y Shen, SJ Callister, JM Jacobs, and RD Smith. 2007. "The Future of Liquid Chromatography-Mass Spectrometry in Metabolic Profiling and Metabolomic Studies for Biomarker Discovery." *Biomarkers in Medicine* 1(1):159-185.
- Palumbo AV, JR Tarver, LA Fagan, MS McNeilly, R Ruther, LS Fisher, and JE Amonette. 2007. "Comparing Metal Leaching and Toxicity from High pH, Low pH, and High Ammonia Fly Ash." *Fuel* 86(10-11):1623-1630.
- Pan D, D Hu, R Liu, X Zeng, S Kaplan, and HP Lu. 2007. "Fluctuating Two-State Light Harvesting in a Photosynthetic Membrane." *Journal of Physical Chemistry C* 111(25):8948-8956.
- Schuchardt KL, BT Didier, T Elsethagen, L Sun, V Gurumoorthi, J Chase, J Li, and TL Windus. 2007. "Basis Set Exchange: A Community Database for Computational Sciences." *Journal of Chemical Information and Modeling* 47(3):1045-1052.
- Shankaran H, H Resat, and HS Wiley. 2007. "Cell Surface Receptors for Signal Transduction and Ligand Transport: A Design Principles Study." *PLoS Computational Biology* 3(6):e101.
- Shin Y, BW Arey, C Wang, XS Li, MH Engelhard, and GE Fryxell. 2007. "Synthesis and Characterization of Phosphate-Coated Mesoporous Titania and Cd-Doping of Same via Ion-Exchange." *Inorganic Chemistry Communications* 10(6):642-645.
- Shin Y, I Bae, BW Arey, and GJ Exarhos. 2007. "Simple Preparation and Stabilization of Nickel Nanocrystals on Cellulose Nanocrystal." *Materials Letters* 61(14-15):3215-3217.
- Smirnov SL, NG Isern, ZG Jiang, DW Hoyt, and CJ McKnight. 2007. "The Isolated Sixth Gelsolin Repeat and Headpiece Domain of Villin Bundle F-Actin in the Presence of Calcium and are Linked by a 40-Residue Unstructured Sequence." *Biochemistry* 46(25):7488-7496.
- Straub TM, K Höner zu Bentrup, P Orosz-Coghlan, A Dohnalkova, BK Mayer, RA Bartholomew, CO Valdez, CJ Bruckner-Lea, CP Gerba, MA Abbaszadegan, and CA Nickerson. 2007. "Cell Culture Assay for Human Noroviruses [response]." *Emerging Infectious Diseases* 13(7):11-17.
- Tarasevich BJ, CJ Howard, JL Larson, ML Snead, JP Simmer, M Paine, and WJ Shaw. 2007. "The Nucleation and Growth of Calcium Phosphate by Amelogenin." *Journal of Crystal Growth* 304(2):407-415.
- Wang CM, DR Baer, JE Amonette, MH Engelhard, Y Qiang, and J Antony. 2007. "Morphology and Oxide Shell Structure of Iron Nanoparticles Grown by Sputter-Gas-Aggregation." *Nanotechnology* 18(25): Art. No. 255603.
- Wang P, O Hadjar, and J Laskin. 2007. "Covalent Immobilization of Peptides on Self-Assembled Monolayer Surfaces Using Soft-Landing of Mass-Selected Ions." *Journal of the American Chemical Society* 129(28):8682-8683.
- Wang Z, X Zu, L Yang, F Gao, and WJ Weber. 2007. "Atomistic Simulations of the Size, Orientation, and Temperature Dependence of Tensile Behavior in GaN Nanowires." *Physical Review. B, Condensed Matter and Materials Physics* 76(4): Art. No. 045310.
- Windisch CF, Jr, DR Baer, RH Jones, and MH Engelhard. 2007. "Electrochemical Effects of S Accumulation on Ion-implanted Alloy 22 in 1 M NaCl Solutions." *Corrosion Science* 49(6):2497-2511.

Wu H, G Liu, J Wang, and Y Lin. 2007. “Quantum-Dots Based Electrochemical Immunoassay of Interleukin-1 $\alpha$ .” *Electrochemistry Communications* 9(7):1573-1577.

Yantasee W, CL Warner, T Sangvanich, RS Addleman, TG Carter, RJ Wiacek, GE Fryxell, C Timchalk, and MG Warner. 2007. “Removal of Heavy Metals from Aqueous Systems with Thiol Functionalized Superparamagnetic Nanoparticles.” *Environmental Science and Technology* 41(14):5114-5119.

Zhang Q, N Tang, JWC Brock, HM Mottaz, JM Ames, JW Baynes, RD Smith, and TO Metz. 2007. “Enrichment and Analysis of Nonenzymatically Glycated Peptides: Boronate Affinity Chromatography Coupled with Electron-Transfer Dissociation Mass Spectrometry.” *Journal of Proteome Research* 6(6):2323-2330.

Zhang Q, W Qian, TV Knyushko, TRW Clauss, SO Purvine, RJ Moore, CA Sacksteder, MH Chin, DJ Smith, DG Camp, II, DJ Bigelow, and RD Smith. 2007. “A Method for Selective Enrichment and Analysis of Nitrotyrosine-Containing Peptides in Complex Proteome Samples.” *Journal of Proteome Research* 6(6):2257-2268.

Zhao H, JE Holladay, H Brown, and ZC Zhang. 2007. “Metal Chlorides in Ionic Liquid Solvents Convert Sugars to 5-Hydroxymethylfurfural.” *Science* 316(5831):1597-1600.

## Presentations

*During this reporting period, EMSL staff presented on research performed at the user facility at the following meetings or locations:*

- 17th International Vacuum Congress (IVC-17), 13th International Conference on Surface Science (ICSS-13), and the International Conference on Nano Science and Technology (ICN+T 2007), July 2, 2007, Stockholm, Sweden.
- 55<sup>th</sup> American Society of Mass Spectrometry Conference, June 4, 2007, Indianapolis, Indiana.
- 62nd Annual Meeting of the Northwest Region of the American Chemical Society, June 18, 2007, Boise, Idaho.
- Fifteenth International Conference on Composites/Nano Engineering (ICCE-15), July 15, 2007, Haikou, China.
- Institute of Electrical and Electronics Engineers (IEEE) 9th International Conference on Inorganic Scintillators and their Applications, June 5, 2007, Winston-Salem, North Carolina.
- Meeting with Department of Homeland Security, July 24, 2007, Arlington.
- Nuclear Magnetic Resonance of Metals in Biological Systems and Materials, June 8-10, 2007, Newark, Delaware.
- Rocky Mountain Analytical Conference, July 21-26, 2007, Breckenridge, Colorado.
- “Remediation of Contaminated Facilities at RRC Kurchatov Institute,” June 5, 2007, Moscow, Russian Federation.

- U.S. Department of Energy Summer School in Multiscale Mathematics and High Performance Computing, June 28, 2007, Corvallis, Oregon.